Insertion Device Magnet Measurements for the Advanced Light Source*

S. Marks, C. Cork, E. Hoyer, D. Humphries, B. Kincaid, D. Plate, A. Robb, R. Schlueter, C. Wang,
Lawrence Berkeley Laboratory, University of California,
1 Cyclotron Road, Berkeley, CA 94720 USA

W. Hassenzahl
Lawrence Livermore National Laboratory, University of California, Livermore, CA 94550 USA

A. Abstract

Allowable magnetic field errors for the 4.6 m long insertion devices for the Advanced Light Source (ALS) are extremely small and are driven by electron beam and radiation requirements. Detailed measurements and adjustments of each insertion device are performed to qualify them for installation in the ALS. To accomplish this, a high speed, precision magnetic measurement facility has been designed and built. Hall probe mapping equipment, capable of completing a 2500 sample, 6 m scan with precision axial position monitoring using a laser interferometer in under one minute, is used to obtain both local and integrated field information. A 5.5 m long, 1 cm wide coil is used to measure the field integral through an entire insertion device. This paper describes magnetic measurement equipment, and results of measurements on IDA, the first of the ALS insertion devices.

I. INTRODUCTION

The ALS is a third generation synchrotron light source designed to produce XUV radiation of unprecedented brightness. To meet the high brightness goal, the storage ring has been designed for very small electron beam emittance, and the insertion devices (IDs) must be built to a high degree of precision. The allowable magnetic field errors are driven by both electron beam and radiation requirements. Detailed magnetic measurements and mechanical adjustments of each ID are performed to qualify it for installation in the ALS. The paper by E. Hoyer [1] et al., describes the first three ALS IDs.

The influence of an ID's magnetic field errors on ALS performance is separated into those that affect spectral brightness of the radiation and those that affect dynamics and life-time of the electron beam. Magnetic field data, consisting of both local field and integral field information, is analyzed to assess these affects. Degradation in spectral brightness is influenced both by systematic and random variations from an ideal periodic field. C. Wang, et al.[2] examines the relationship between magnetic errors and spectral performance. The primary influence on the electron beam is due to errors in the integrated magnetic field.

Primary magnetic field data is derived from Hall probe measurements. This data allows examination of both local and integral field characteristics. In addition, a field integral can be separated into the contribution due to errors in the periodic middle section, and the contributions from each end. These data provide a prescription for nulling the first and second field integrals, which affect electron beam steering. A system of dual permanent magnet rotors is included in the end structure for this purpose [3]. In addition to Hall probe measurements, full field integrals are also measured with a 5.5 m long integral coil, which confirms integrated Hall probe data.

II. MAGNET MEASUREMENT FACILITY

B. Hall Probe Measurement System — Mechanical

Figure 1 is a photograph of the "Luge", a custom built stage which translates axially (z) through the gap of an ID. Probes are mounted to a light weight plastic platform on the Luge. Horizontal (x) and vertical (y) probe position can be varied, via micro-stepping motors which move the support platform. Support for the Luge is provided by a rail on the one side of the gap and a pneumatic cylinder on the other. The cylinder and rail are mounted directly to the ID support structure. The pneumatic cylinder provides the mechanism for axial translation.

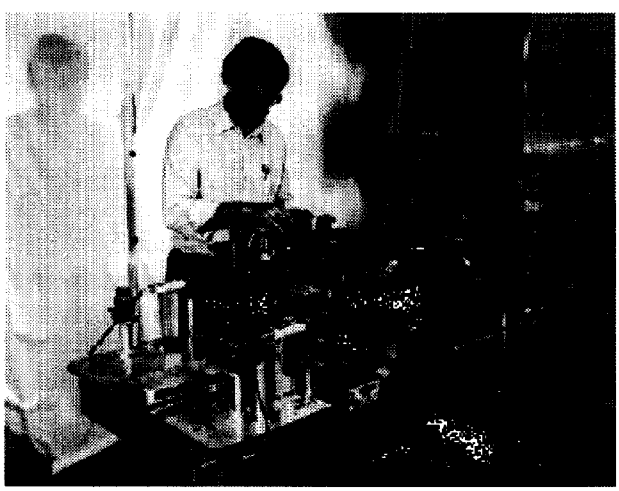

Figure 1. Photograph of "Luge."

Accurate axial position monitoring of the Luge is accomplished with a resolution of 1 μm using a dual beam laser interferometer system. Two retro-reflectors mounted to the Luge provide interferometer beam targets. They are mounted over the pneumatic cylinder and over the track and correspond to interferometer channels 1 and 2, respectively.

C. Electronics

Design of the instrumentation system is based upon use of a dedicated subsystem for real-time instrument control along

*This work was supported by the Director, Office of Energy Research, Office of Basic Energy Sciences, Material SciencesDivision of the U.S. Department of Energy under Contract No. DE-AC03-76SF00098.

0-7803-1203-1/93$03.00 © 1993 IEEE

with a separate workstation for measurement coordination and data reduction and storage. The computer and electronics used for instrument control and data acquisition are schematically illustrated in Figure 2.

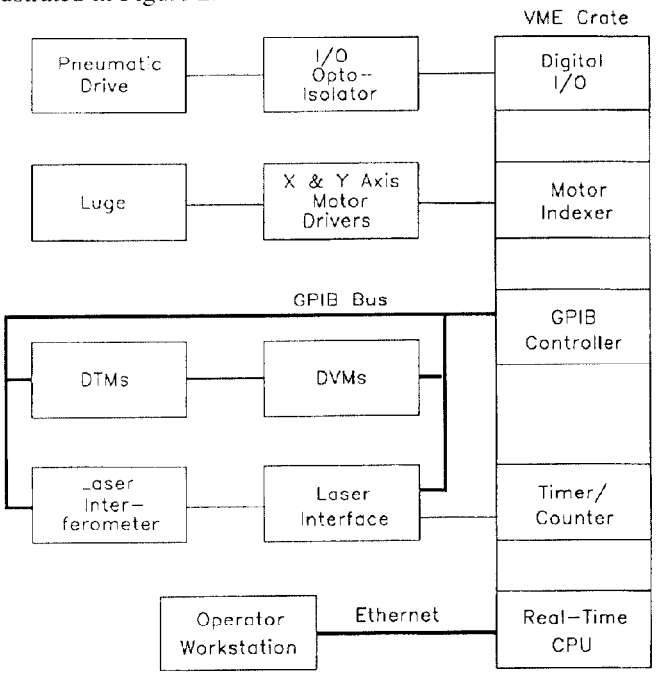

Figure 2. Block diagram of instrumentation.

The electronics rack contains various instruments and a real-time subsystem for fast data collection and instrument control. The equipment includes a VME crate, two Hewlett Packard 3458A digital voltmeters (DVMs), two Compumotor LN-Series micro-stepper motor drivers, an LBL-designed opto-isolator interface chassis, a ZYGO Axiom 2/20 laser interferometer system, and two Group 3 DTM-141-DG digital tesla meters (DTMs). The VME crate includes a Motorola-147S real time central processing unit (CPU), a Burr Brown MPV991 timer/counter module, a Motorola MVME-300 GPIB instrument bus controller, an Oregon Microsystems VME-44 four channel stepper motor indexer, and a VMIC VMIVME-2534 digital input/output module. An LBL-designed electronics chassis interfaces the timer/counter module with the laser interferometer and DVMs.

The MVME-147S provides real-time data collection and instrument control. DVMs sample Hall probe analog output voltages, corresponding to B_y and B_x, and store the data in internal memory. Sampling occurs when triggers are received from the timer/counter module, which processes output data from channel 1 of the laser interferometer. The laser interferometer is set to provide pulses, in A-quad-B format, at 1 μm scan increments. The timer/counter provides triggers at 0.1 mm increments. The timer/counter module also measures the time interval between samples and the motion increment of interferometer channel 2. This allows for correction of measurement position.

The operator workstation includes a Sun IPC workstation and an non-interruptable power supply. The workstation provides a user interface and facilities for data reduction and storage.

The DVMs, laser interferometer, and Hall probes are controlled via GPIB. Communication between the MVME-147S and the Sun IPC occurs via an Ethernet interface.

D. Data Acquisition Software

Coordination between the real-time subsystem and the workstation is based upon a client/server model. Software running on the workstation provides basic coordination of measurements; this software acts as a client which requests service from the real-time instrument control software running on the VME crate. Communication between the subsystems is provided by the Sun remote procedure call (RPC) mechanism.

There is a close correspondence between software modules of the real-time subsystem and hardware components within the electronics rack. Software modules *Dvm*, *Dtm*, and *Laser* control the DVMs, DTMs, and laser interferometer, respectively. Each software module communicates with its respective instrument via a GPIB bus interface. Communication is handled by *Mv300*, which controls the MVME-300 GPIB interface board. Software modules *Mv2534* and *Mv44* control the VMIVME-2534 digital I/O board and the VME-44 motor indexer, respectively. *Mv2534* and *Mv44* are interfaced to the *Stage* module which controls probe position and axial translation of the Luge. The device handler *Mpv991* provides services for access and control of the parallel counter channels and the interrupt controller of the MPV991 timer/counter board. The *Counter* module configures *Mpv991* specifically for the field map measurements.

Scan_svc is the top level server task on the real-time subsystem, providing remote procedure call service to client tasks. *Scan_svc* is spawned during system initialization and listens to the network for service requests. *Scan_clnt* is the client interface module. It resides on the operator workstation as a subroutine library that coordinates network connections, RPC access, and disconnection to the server module. *ID_scan* runs on the operator workstation and provides basic coordination of a field scan. A set of additional utility routines also exist for single value DVMread (*readDVM*), single value DTM read (*readDTM*), Luge motion control (*homeXY*, *moveX*, *moveY*, and *launchZ*), and ID gap control (*initGap* and *moveGap*). Each utility routine calls *Scan_clnt* for access to the device control subroutines. A Unix script routine, *multiScans*, is a user interface which provides a mechanism for the definition and automated control of a set of field scans.

E. Data Reduction Software

A raw data file consists of a header including measurement parameter settings and the following values for each data sample: Hall probe voltage, interferometer channel 1 counts, interferometer channel 2 counts, and time interval between samples. Program *Convert* creates a first level reduced data file consisting of (z, B_y) pairs for each data sample. Input for *Convert* consists of a Hall probe conversion table file and a raw data file. A Hall probe conversion table consists of corre-

sponding values of output voltage and magnetic field. The B_y value is calculated by linear interpolation of the conversion table. Note that the conversion table is preprocessed using a spline routine to create a dense mesh of voltage-magnetic field pairs; this allows an efficient and accurate conversion.

The axial position z is calculated from interferometer count and timer information according to the following equation

$$z = \frac{n_1(X_1 - x) + n_2(X_2 - x)}{X_1 + X_2} + v\tau/2$$

where n_1 and n_2 are counts from interferometer channels 1 and 2, respectively, x is the horizontal probe position relative to a horizontal datum, X_1 and X_2 are the horizontal distances between retro-reflectors 1 and 2, respectively, and the horizontal datum, v is the probe velocity, and τ is the DVM integration time.

Higher level data reduction is performed on the converted file using a set of utilities included in program *analyze* [4]. This program includes utilities for spline fit of a data set, calculation of deviation from an ideal periodic field, Fourier transform of data, and calculation of the optical phase and radiation spectrum.

IV. RESULTS

Figure 3 shows a Fourier transform of a magnetic field scan from IDA. The large spectral peaks at odd harmonic numbers is characteristic of the periodic magnetic field of an insertion device. This figure also illustrates the signal to noise level achieved in the measurement system. The background spectrum at the right side of the graph indicates the level of random measurement noise. Note that this is at a level of less than 1×10^{-5} relative to the first harmonic. In other words, the measured value of peak fields is 1×10^{5} times larger than the noise level.

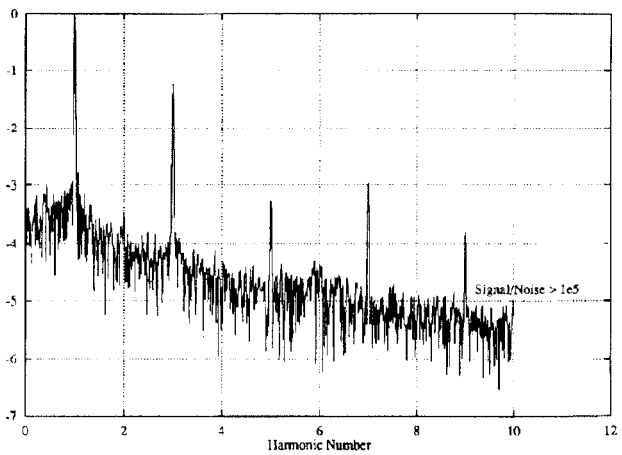

Figure 3. Fourier transform of B_y scan.

Figure 4 shows the results of a series of measurements of $\int B_y \cdot dz$ at different x locations within the range ± 30 mm and at 14 mm and 23 mm ID gaps. Integrals are shown both for integrated Hall probe scans and integral coil measurements. Note that the agreement between the two methods of integral measurement is quite good. The graph also illustrates the level of uniformity that was achieved in $\int B_y \cdot dz$ as a function of x; nonuniformity in this function affects electron beam dynamics.

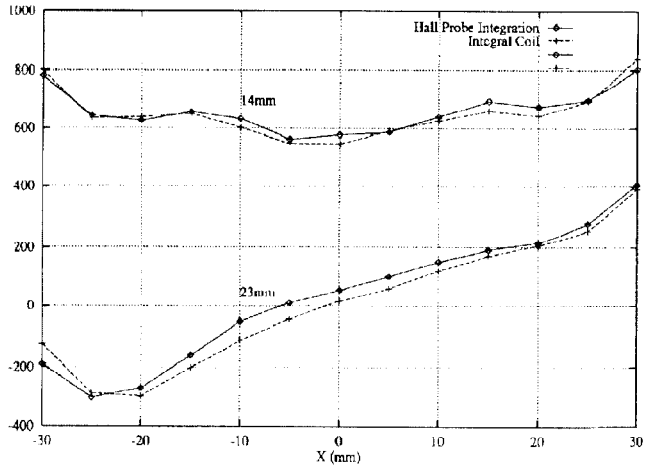

Figure 4. $\int B_y \cdot dz$ as a function of x.

V. CONCLUSIONS

The insertion device magnetic measurement system described in this paper has proven to be very efficient and reliable. The mechanisms for rapid compilation and analysis of data has allowed for an extensive characterization of ALS insertion devices. To date, over 2 GB of magnetic scan data have been collected, and the luge has logged over 25 km of travel.

VI. REFERENCES

[1] E. Hoyer, J. Akre, J. Chin, B. Gath, D. Humphries, B. Kincaid, S. Marks, P. Pipersky, D. Plate, G. Portmann, R. Schlueter, W.V. Hassenzahl, "First Undulators for the Advanced Light Source," IEEE PAC (May 1993)

[2] C. Wang, S. Marks, B. Kincaid, "Spectral Quality of ALS U5.0 Undulator and Field Error Effects," IEEE PAC (May 1993)

[3] D. Humphries, K. Halbach, E. Hoyer, B. Kincaid, S. Marks, R. Schlueter, "Modeling and Measurement of the ALS Undulator End Magnetic Structures," IEEE PAC (May 1993)

[4] J. Bahrdt, B. Kincaid, W. Hassenzahl, "ANALYZE, A Program for the Analysis of Magnetic Field Data."